Geomechanics and Engineering, *Vol. 15, No. 3 (2018) 919-925*
DOI: https://doi.org/10.12989/gae.2018.15.3.919

Applicability of exponential stress-strain models for carbonate rocks

Vyacheslav Palchik*

Department of Geological and Environmental Sciences, Ben-Gurion University, POB 653, Beer-Sheva 84105, Israel

(Received June 3, 2017, Revised January 18, 2018, Accepted March 23, 2018)

Abstract. Stress-strain responses of weak-to-strong carbonate rocks used for tunnel construction were studied. The analysis of applicability of exponential stress-strain models based on Haldane's distribution function is presented. It is revealed that these exponential equations presented in transformed forms allow us to predict stress-strain relationships over the whole pre-failure strain range without mechanical testing of rock samples under compression using a press machine and to avoid measurements of axial failure strains for which relatively large values of compressive stress are required. In this study, only one point measurement (small strain at small stress) using indentation test and uniaxial compressive strength determined by a standard Schmidt hammer are considered as input parameters to predict stress-strain response from zero strain/zero stress up to failure. Observations show good predictive capabilities of transformed stress-stress models for weak-to-strong (σ_c <100 MPa) heterogeneous carbonate rocks exhibiting small (< 0.5 %), intermediate (< 1 %) and large (> 1 %) axial strains.

Keywords: stress-strain model; failure strain; uniaxial compressive strength; carbonate rocks

1. Introduction

The overburden rock behavior under compression plays a decisive role for tunnel stability. The prediction of stress-strain responses of rocks under compression is important for the definition of Young's modulus and stress and strain values at different stages of mechanical behavior of different rocks from zero strain/zero stress up to failure. A lot of researches (Kodner 1963, Duncan and Chang 1970, Haas 1989, Tatsuoka and Shibuya 1992, Tharp and Scarbrough 1994, Muravskii 1996, Puzrin and Burland 1996, Ching *et al*. 1997, Fairhurst and Hudson 1999, Gutierrez *et al*. 2000, Shibuya 2002, Habimana *et al*. 2002, Palchik 2006, 2007, Liu *et al*. 2009, Garaga and Latha 2010, Palchik 2012, Bogusz and Bukowska 2015) were focused on the modeling of stress-strain response of soils and rocks under compression. Stress-strain models (e.g., Kodner 1963, Duncan and Chang 1970, Haas 1989, Tatsuoka and Shibuya 1992, Tharp and Scarbrough 1994, Puzrin and Burland 1996, Fairhurst and Hudson 1999, Gutierrez *et al*. 2000, Shibuya 2002, Habimana *et al*. 2002) traditionally use normalized axial stress and strain values and require a certain number of unknown constants. The larger the number of unknown constants, the larger the number of data points over the pre-failure strain range needed for representing the stress-strain relationship.

Hyperbolic (Kodner 1963, Duncan and Chang 1970, Tharp and Scarbrough 1994, Habimana *et al*. 2002), logarithmic (Puzrin and Burland 1996), double exponential (Shibuya 2002) and exponential (Palchik 2006, 2012) stress-strain models for different rock types have been proposed. Mathematical forms of the models (Tatsuoka and Shibuya 1992, Puzrin and Burland 1996, Shibuya 2002, Palchik 2006, 2012) which provide a better approximation of stress-strain data over the whole pre-failure strain range, and constants and parameters involved in these models are discussed in detail elsewhere (Palchik 2006, 2012). Note that the stress-strain models proposed by Tatsuoka and Shibuya (1992), Puzrin and Burland (1996), Shibuya (2002) are suitable only for rocks exhibiting small (ε_{af} < 0.5 %) failure strains. Kumara and Hayano (2016) have found deformation characteristics of crushed stone-sand mixtures, simulating fresh and fouled ballasts. Effect of particle shape on stress-strain behaviour of these mixtures is revealed. Yadollahia and Benli (2017) have studied stress-strain behavior of geopolymers: it is established how different fineness, mix design and curing method influence on geopolymer stress-strain response. Li *et al.* (2018) have conducted uniaxial loading cycle tests on the coal rock in order to study the rock dilatation at different loading rates.

Palchik (2006, 2012) has proposed exponential stress-strain models based on Haldane's distribution function for weak-to-strong (σ_c < 100 MPa) heterogeneous carbonate rocks (chalks, dolomites and limestones) exhibiting small (ε_{af} < 0.5 %), intermediate ($\varepsilon_{af} \leq$ 1 %) and large (ε_{af} > 1 %) axial failure strains. To obtain accurate stress-strain relationship over the whole pre-failure strain range with the proposed stress-strain models, it is necessary to have only one datum point (uniaxial compressive strength (σ_c) and axial failure strain (ε_{af}) at this strength). Unfortunately, erroneous opinion that ε_{af} and σ_c required for these models can be determined only by defining the whole stress-strain curve from zero strain/zero stress to failure using a press machine leads to a limited use of these useful models in engineering practice.

The goal of this paper is to argue that these exponential equations (Palchik 2006, 2012) presented in transformed

*Corresponding author, Ph.D.
E-mail: vplachek@bgu.ac.il

ISSN: 2005-307X (Print), 2092-6219 (Online)

forms allow one to avoid the measurement of axial failure strain (ε_{af}) and the mechanical testing of rock samples under compression using a press machine. The applicability of transformed stress-strain models for accurate prediction of stress-strain responses of heterogeneous carbonate rocks over the whole pre-failure strain range is analyzed.

The novelty of the presented work as compared to papers published earlier (Palchik 2006, 2012) is the mathematical formulation of exponential stress-strain models which do not require the measurement of axial failure strain, argumentation of the choice of equations required for the prediction of stress-strain responses of carbonate rocks exhibiting different levels of axial failure strain, and detailed examination of proposed stress-strain models taking in account the most unfavorable points of stress-strain curves, where the values of relative errors are maximum.

2. Background

Palchik (2006, 2012) has recently created the following two exponential stress-strain models based on Haldane's distribution function for heterogeneous carbonate rocks

$$\frac{\sigma_a}{\sigma_c} = \frac{1 - e^{-2\varepsilon_a}}{1 - e^{-2\varepsilon_{af}}} \tag{1}$$

$$\frac{\sigma_a}{\sigma_c} = \frac{1 - e^{-k_1 \varepsilon_a \varepsilon_{af}^{-k_2}}}{1 - e^{-k_1 \varepsilon_{af}^{1-k_2}}} \tag{2}$$

where σ_a/σ_c is a normalized axial stress; σ_a (MPa) is a current axial stress; σ_c (MPa) is an uniaxial compressive strength; ε_a(%) is a current axial strain; ε_{af} (%) is an axial failure strain at σ_c; the constant 2 in Eq. (1) is a constant involved in the canonical form of Haldane's function (Haldane 1919). In Eq. (2), k_1 and k_2 are statistical coefficients used instead of the constant equal to 2: k_1 = 1.63, k_2 = 1.1 for carbonate rocks.

It is obvious from Eqs. (1) and (2) that when $\varepsilon_a = 0$, the value of σ_a/σ_c is zero. When $\varepsilon_a = \varepsilon_{af}$, the value of σ_a/σ_c becomes equal to 1. All parameters (ε_a, σ_a, ε_{af} and σ_c) involved in Eqs. (1) and (2) are shown in Fig. 1. It should be noted that Eq. (1) is suitable for carbonate rocks exhibiting small ($\varepsilon_{af} < 0.5$ %) and intermediate failure strains ($\varepsilon_{af} \leq 1$ %), whereas Eq. (2) is suitable for those having large axial failure strains ($\varepsilon_{af} > 1$ %). The calculated normalized axial stress/axial strain curves for different levels of failure strain ε_{af} = 0.2%, 0.4 %, …., 1 % (Eq.(1)) and ε_{af} = 1.2 %, 1.4 %, … , 2.8 % (Eq.(2)) are presented in Fig. 2. Here all stress-strain curves are slightly concave upwards with a different degree of non-linearity. The latter is increased with growing axial strain.

The exponential stress-strain models (Eqs. (1) and (2)) based on Haldane's distribution function provide a better approximation of stress-strain data for weak-to-strong ($\sigma_c <$ 100 MPa) heterogeneous carbonate rocks. As stated earlier, only one datum point (σ_c and ε_{af} at this σ_c) is needed to predict the stress-strain relationship over the entire pre-failure strain range.

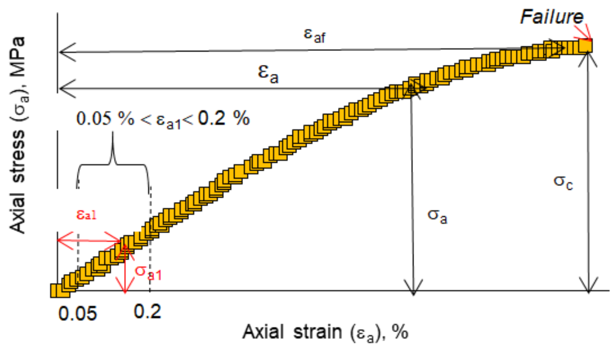

Fig. 1 Stress and strain parameters: σ_a and ε_a are current axial stress and strain, respectively; σ_c is uniaxial compressive strength, ε_{af} is axial failure strain (at σ_c) involved in Eqs. (1) and (2); ε_{a1} =0.05 % - 0.2 % and σ_{a1} is one point measurement used as input parameter in Eqs. (13) and (15)

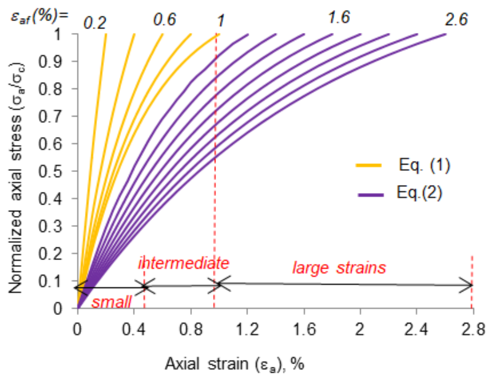

Fig. 2 Calculated normalized axial stress-axial strain relations for different levels of axial failure strain (0.2 % < ε_{af} < 2.8 %)

In this study, the author intends to present Eqs. (1) and (2) in a more efficient manner, in which one point measurement (small strain at small stress) is used instead of the final point (σ_c and ε_{af} at this σ_c) of pre-failure strain range. Such transformation allows us to avoid the measurement of axial failure strain (ε_{af}) and uniaxial compressive strength (σ_c) in press machine for compressive testing.

3. Test procedure

Stress-strain responses of different heterogeneous carbonate rocks were observed at the Rock Mechanics Laboratory of the Ben-Gurion University. Chalk, dolomite and limestone samples exhibiting wide ranges of axial failure strains (0.13 % < ε_{af} < 2.75 %), elastic modulus (6200 MPa < E < 56000 MPa), Poisson's ratio (0.13 < ν < 0.49) and dry bulk density (1.6 g/cm^3 < ρ < 2.7 g/cm^3) were collected from different regions of Israel (Palchik 2006, 2007, 2012). Rock samples were prepared following ISRM suggested methods with NX size (diameter of 54 mm and length/diameter ratio of 2). The samples were ground to the

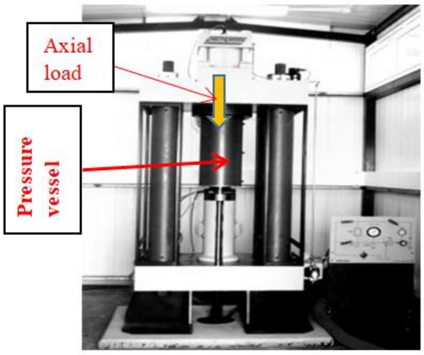

Fig. 3 Load frame (TerraTek system, model FX-S-33090)

planeness of 0.0 1mm and cylinder perpendicularity within 0.05 radians. All samples were oven dried at the temperature of 110°C for 24h. The selected rock samples were free of cracks, fissures and veins, which would act as planes of weakness and exert an undesirable effect on stress-strain curves. The studied rock samples may be described according to the ISRM suggested methods (Brown 1981) as weak ($5 < \sigma_c < 25$ MPa), medium strong ($25 < \sigma_c < 50$ MPa) and strong ($50 < \sigma_c < 100$ MPa).

The load frame used in this study (TerraTek system, model FX-S-33090) operates under hydraulic closed-loop servo-control with a maximum axial force of 1.4 MN and load frame stiffness of 5×10^9 N/m. The load was measured by a sensitive load cell located in series with the sample having the maximum capacity of 1000 kN and the linearity of 0.5% of full scale. The axial strain cantilever set has a 10% strain range, and the radial strain cantilevers have a strain range limit of 7%, with the linearity of 1% for the full scale in both sets. The load frame and sample with radial and axial cantilever sets are described in detail elsewhere (Palchik and Hatzor 2000, Palchik 2014). All samples were tested at a constant strain rate of 10^{-5} /s and at the ambient temperature of 25°.

The load frame is presented in Fig. 3. Axial load is applied by means of a servo-controlled actuator on the load frame. The rock sample is located inside the pressure vessel. Prior to testing, each sample was jacketed in a shrink tube to isolate the rock material from the pressure vessel oil even when the pressure in the vessel was zero during the test (uniaxial compression). Axial and radial strains were measured in three orthogonal directions using axial and radial strain cantilevers. These cantilevers are located on the rock sample subjected to uniaxial compression.

4. Transformation of stress-strain models

The models given by Eqs. (1) and (2) relate the axial stress (σ_a) to uniaxial compressive strength (σ_c) and exponential function, where the exponent is the axial strain (ε_a). Eqs. (1) and (2) can be rewritten as the following two mathematical expressions for $\varepsilon_{af} < 1$ % and $\varepsilon_{af} > 1$ %, respectively

$$F_i = \frac{1-e^{-2\varepsilon_{ai}}}{\sigma_{ai}} = \frac{1-e^{-2\varepsilon_{a1}}}{\sigma_{a1}} = \frac{1-e^{2\varepsilon_{a2}}}{\sigma_{a2}},...,= \frac{1-e^{-2\varepsilon_{an}}}{\sigma_{an}} \quad (3)$$

$$D_i = \frac{1-e^{-k_1\varepsilon_{ai}\varepsilon_{af}^{-k_2}}}{\sigma_{ai}} = \frac{1-e^{-k_1\varepsilon_{a1}\varepsilon_{af}^{-k_2}}}{\sigma_{a1}} = \frac{1-e^{-k_1\varepsilon_{a2}\varepsilon_{af}^{-k_2}}}{\sigma_{a2}},...,= \frac{1-e^{-k_1\varepsilon_{an}^{1-k_2}}}{\sigma_{an}} \quad (4)$$

where $i = 1, 2, \ldots, n$ are the number of points on stress-strain curve where the axial stress and axial strain were measured; $\sigma_{ai} = \sigma_{a1}, \sigma_{a2}, \ldots, \sigma_{an}$ are axial stresses measured in points 1, 2, ..., n, respectively; $\varepsilon_{ai} = \varepsilon_{a1}, \varepsilon_{a2}, \ldots, \varepsilon_{an}$ are axial strains measured at $\sigma_{a1}, \sigma_{a2}, \ldots, \sigma_{an}$, respectively, in points 1, 2, ..., n, respectively; n is the final point of pre-failure strain range, where σ_c and ε_{af} at σ_c were measured, i.e. $\varepsilon_{an} = \varepsilon_{af}$ is the axial failure strain and $\sigma_{an} = \sigma_c$ is the uniaxial compressive strength.

In order to avoid the measurement of axial failure strain (ε_{af}), the latter must be calculated. Now the author attempts to show how the above-mentioned expressions (Eqs. (3) and (4)) can be used for the calculation of ε_{af} in terms of σ_c and only one point measurement (σ_{a1} and ε_{a1} at σ_{a1}). To calculate the ε_{af} value using σ_c, ε_{a1} and σ_{a1}, Eq. (3) and Eq. (4), respectively, can be reduced to

$$\frac{1-e^{-2\varepsilon_{a1}}}{\sigma_{a1}} = \frac{1-e^{-2\varepsilon_{af}}}{\sigma_c} \quad (5)$$

$$\frac{1-e^{-k_1\varepsilon_{a1}\varepsilon_{af}^{-k_2}}}{\sigma_{a1}} = D_n \quad (6)$$

where $D_n = B/\sigma_c$, and the value of B is defined as

$$B = 1-e^{-k_1\varepsilon_{af}^{1-k_2}} \quad (7)$$

The value of B insignificantly decreases from 0.8 to 0.77 with an average value of 0.78 when ε_{af} increases from 1 % to 2.75 %. Since standard deviation of the average B is small (only 0.0075), we can use an average value of B = 0.78 for further calculation.

The axial failure strain (ε_{af}) can be obtained from Eqs. (5) and (6), respectively, as

$$\varepsilon_{af} = -0.5\ln\left(1-\sigma_c F_1\right) \quad (8)$$

$$\varepsilon_{af} = A^{\frac{1}{k_2}} \quad (9)$$

where F_1 and A are computed according to the following mathematical expressions

$$F_1 = \frac{1-e^{-2\varepsilon_{a1}}}{\sigma_{a1}} \quad (10)$$

$$A = -\frac{k_1\varepsilon_{a1}}{\ln(1-\frac{B\sigma_{a1}}{\sigma_c})} \quad (11)$$

Taylor series expansion (Hazewinkel 2001) of the logarithmic expressions of $\ln(1-\sigma_c F_1)$ and $\ln(1- B\sigma_{a1}/\sigma_c)$ involved in Eqs. (8) and (11), respectively, is the following

$$\ln(1-x) = -\sum_j^{\infty}\frac{x^j}{j} \approx -\left(x+\frac{x^2}{2}+\frac{x^3}{3}\right) \quad (12)$$

where $x = \sigma_c F_1$ and $B\sigma_{a1}/\sigma_c$ for Eqs. (8) and (11), respectively.

Substitution of Eqs. (8) and (12) into Eq. (1) yields a model calculation of stress-strain relationship for rocks exhibiting $\varepsilon_{af} < 1$ %, and this model presented in terms of σ_c, σ_{a1} and ε_{a1} has the following form

$$\sigma_a = \sigma_c\left(\frac{1-e^{-2\varepsilon_a}}{1-e^{-\varsigma}}\right) \tag{13}$$

where the exponent ς is computed as

$$\varsigma = \mu + \frac{\mu^2}{2} + \frac{\mu^3}{3} \tag{14}$$

where $\mu = \sigma_c F_1$.

Combination of Eqs. (2), (9) and (12) gives a model calculation of stress-strain relationship for rocks having $\varepsilon_{af} > 1$ %. The model is also written in terms of σ_c, σ_{a1} and ε_{a1} as

$$\sigma_a = \sigma_c\left(\frac{1-e^{-\lambda\varepsilon_a}}{1-e^{-c\delta}}\right) \tag{15}$$

where $c = k_1^{1/k2} = 1.56$ and parameters of λ and δ are defined as

$$\lambda = \eta\varepsilon_{a1}^{-1} \tag{16}$$

$$\delta = \left(\frac{\varepsilon_{a1}}{\eta}\right)^d \tag{17}$$

where $d = (1/k_2)-1 = -0.091$, and the parameter η involved in Eqs. (16) and (17) is defined as

$$\eta = B\omega + \frac{B^2\omega^2}{2} + \frac{B^3\omega^3}{3} \tag{18}$$

where $\omega = \sigma_{a1}/\sigma_c$.

Since $B = 0.78$, Eq. (18) can be rewritten as

$$\eta = 0.78\omega + 0.304\omega^2 + 0.158\omega^3 \tag{19}$$

5. Examination of proposed stress-strain model

Eqs. (13) and (15) obtained as a result of transformation of Eqs. (1) and (2), respectively, allow us to determine stress-strain relations without measurements of axial failure strain (ε_{af}). The equations (Eqs. (8) and (9)) used for the development of Eqs. (13) and (15), respectively, are mathematically justified, since they return the failure strain (ε_{af}) if the failure data ($\varepsilon_{a1} = \varepsilon_{af}$ and $\sigma_{a1} = \sigma_c$) are used as input values. Indeed, Eq. (8) returns ε_{af} in case of $\varepsilon_{a1} = \varepsilon_{af}$ and $\sigma_{a1} = \sigma_c$, as demonstrated by the following expression

$$\varepsilon_{af} = -0.5\ln\left[1-\frac{\sigma_c\left(1-e^{-2\varepsilon_{af}}\right)}{\sigma_c}\right] = \varepsilon_{af} \tag{20}$$

Eq. (9) also returns ε_{af} in case where $\varepsilon_{a1} = \varepsilon_{af}$ and $\sigma_{a1} = \sigma_c$. For example, when $\varepsilon_{a1} = \varepsilon_{af} = 2\%$ (at $\sigma_{a1} = \sigma_c$), the result of calculation according to Eq. (9) is also equal to 2%

$$\varepsilon_{af} = \left[-\frac{1.63\times 2}{\ln(1-0.78)}\right]^{\frac{1}{1.1}} = 2\,\% \tag{21}$$

Fig. 4 confirms that the input and calculated values of ε_{af} are equal: linear fit exhibits $R^2 = 0.99$ and slope = 0.99.

In Fig. 4, x-axis shows the input values of $\varepsilon_{a1} = \varepsilon_{af} = 1\%$, 1.05 %, 1.1 %, … , 2.75 %, while y-axis shows the values of ε_{af} calculated according to Eq. (9) for each input value of $\varepsilon_{a1} = \varepsilon_{af}$.

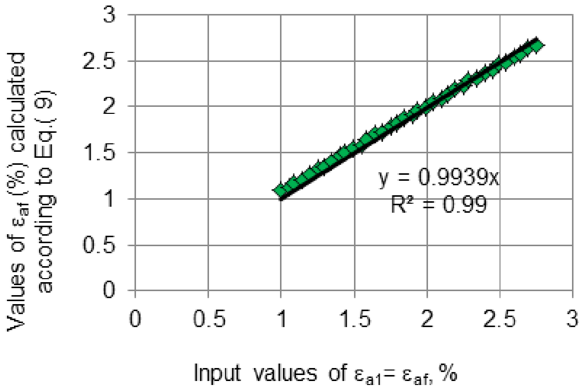

Fig. 4 Linear relation ($R^2 = 0.99$ and slope = 0.99) between input values of $\varepsilon_{a1} = \varepsilon_{af} = 1\%$, 1.05%, 1.1%, … , 2.75 % and values of ε_{af} calculated according to Eq. (9)

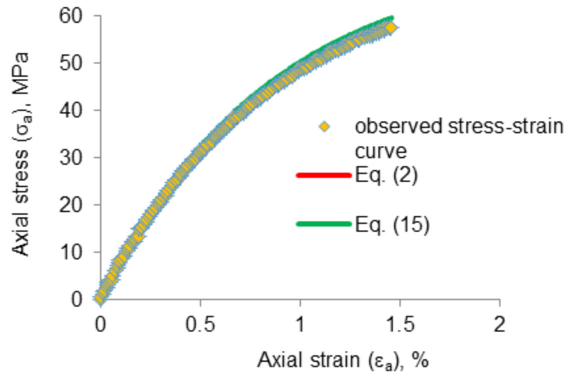

(a) Calculated (Eqs. (2) and (15)) and observed stress-strain curves

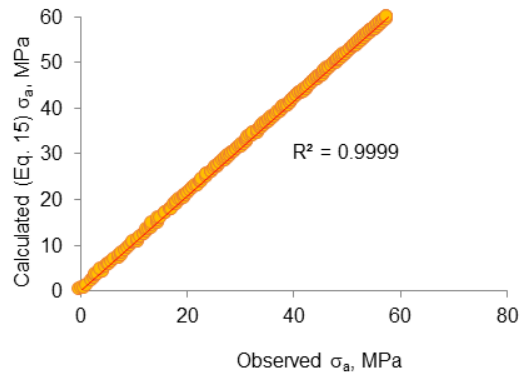

(b) Linear correlation (R^2 =0.99) between calculated (Eq. 15) and observed σ_a

Fig. 5 Comparison between calculated and observed stress-strain relations

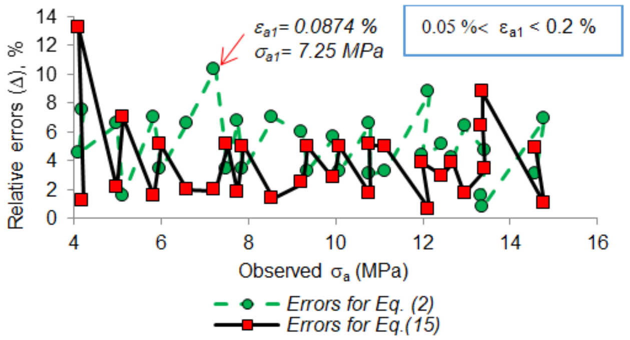

Fig. 6 Sample 4U: Relative errors between observed and calculated (Eqs. 2 and 15) values of σ_a

The comparison between computed (according to Eqs. (13) and (15)) and observed stress-stress curves shows that these curves are very close to each other. The comparison was performed for 55 rock samples (8 chalk, 4 limestone and 4 dolomite formations) studied by Palchik (2006, 2012). The names of carbonate formations and all 55 rock samples, as well as stress and stress characteristics of each rock sample, are presented in detail elsewhere (Palchik 2006, 2012). Moreover, the comparison of the observed and calculated stress-strain curves was performed for 10 new rock samples (Meishash limestone and chalk and Bina limestone) that were not earlier involved in the creation of stress-strain models (Eqs. (1) and (2)) based on Haldane's distribution function (Palchik 2006, 2012). Example of comparison between calculated (Eqs. (2) and (15)) and observed stress-strain relations for new chalk sample 4U (σ_c = 57.7 MPa, ε_{af} = 1.46%) exhibiting ε_{af} > 1% is presented in Fig. 5. The latter shows good linear correlation (R^2 = 0.999) between the observed and calculated (Eq.(15)) values of σ_a. The calculation according to Eq. (15) was performed taking in account the most unfavorable point (ε_{a1} = 0.0874% at σ_{a1} = 7.25 MPa) in Fig. 6, where the value of relative error (Δ) for Eq. (2) is maximum (Δ = 10.37%).

Even in this unfavorable case, relative errors for Eq. (15) graphically presented in Fig. 6 are less than 15%. Thus, predictive capability of the proposed stress-strain model (Eq. (15)) is good. In order to calculate σ_a value according to Eqs. (13) and (15) proposed in this study, only one datum point (ε_{a1} and σ_{a1}) should be selected over the specific strain range. Palchik (2007) has found that the value of ε_{a1} must be larger than 0.05%, since very small strain (ε_{a1} < 0.05%) gives large relative errors (Δ > 20%) at the calculation of axial stress. On the other hand, analysis of stress-strain curves for rock samples exhibiting ε_{af} > 1% shows that ε_{a1} should be smaller than 0.2% in order to avoid calculation errors. Thus, strain range where one datum point (ε_{a1} and σ_{a1}) should be selected is 0.05%-0.2 %, as shown in Fig. 1. For this reason, Fig. 6 presents values of Δ for 0.05% < $\varepsilon_{a1} \leq$ 0.2%.

6. Discussion

The proposed mathematical apparatus (Eqs. (13) and (15)) was successfully used to calculate the stress-strain responses of weak-to-strong (σ_c < 100 MPa) carbonate rocks exhibiting small, intermediate and large axial strains. Calculation of stress-strain curve according to Eqs. (13) and (15) is possible when the uniaxial compressive strength (σ_c) and only one datum point (σ_{a1} and ε_{a1} at this σ_{a1}) are known a priori. It is important to note that these input parameters (σ_c, ε_{a1} at σ_{a1}) can be defined without the mechanical testing of rock samples under compression using a press machine and the definition of the whole stress-strain curve from zero strain/zero stress to failure needed for determining the failure strain. Indeed, the values of σ_c, and ε_{a1} at σ_{a1} can be tested using portable devices, and these tests are much easier, quicker and more economical to use than uniaxial compressive strength test. The value of σ_c can be determined by a standard Schmidt hammer (Schmidt 1951, ASTM 2001, Karaman and Kesimal 2015) which is a non-destructive, portable and cost-effective device for hardness testing. Schmidt hammer test is based on the rebound of a steel hammer from the rock surface, which is proportional to the compressive strength of the rock surface.

The values of σ_{a1} and ε_{a1} at σ_{a1} are measured using indentation test by forcing indenters of various shapes into the tested rock sample under controllable indenter displacement and applied force (Chen and Labuz 2006, Haftani *et al*. 2013, Kalyan *et al*. 2015).

In the paper, two sets of equations were proposed: one for small and intermediate failure strains and another for large failure strain. The choice of equations for rock samples exhibiting different levels of axial failure strains is performed using Eqs. (8), (9) and Fig. 2. There are three input parameters (0.05 % <ε_{a1}< 0.2 %, σ_{a1} at this ε_{a1}, and σ_c) measured using portable devices. These parameters are used for the calculation of failure strain (ε_{af}) according to Eqs. (8) and (9). Eq. (8) is suitable for rocks exhibiting small and intermediate failure strains (< 1%), whereas Eq. (9)-for large failure strains (> 1%). Values of ε_{af} were computed according to Eqs. (8) and (9) for all 65 rock samples. Then the calculation results were compared with the results presented in Fig. 2. It was established that when the value of ε_{af} calculated according to Eq. (9) for any rock sample is smaller than 1% (and, therefore, is not valid), the value of 0.2% < $\varepsilon_{af} \leq$ 1% calculated according to Eq. (8) for the same sample is consistent with the value of ε_{af} presented in Fig. 2 and, hence, stress-strain model (Eq. (13)) for small and intermediate failure strains should be chosen. On the other hand, when the value of ε_{af} calculated according to Eq. (9) is between 1% and 2.8%, this value is confirmed by Fig. 2 and, therefore, stress-strain model (Eq. (15)) proposed for large strains is chosen.

Thus, the use of proposed models (Eqs. (13) and (15)) allows us to avoid mechanical testing of rock samples under compression using a press machine. It is not necessary to measure axial failure strain. Note that it is sufficient to apply only one stress level (σ_a = σ_{a1}) by forcing indenter into the sample and to define a small value of 0.05% < ε_a = ε_{a1} < 0.2% only at this σ_a = σ_{a1}. The applied stress of σ_a = σ_{a1} is significantly lower than uniaxial compressive strength (σ_c) at which the failure occurs. Uniaxial compressive strength is measured by non-destructive method (Schmidt hammer) and, therefore, the same unbroken rock sample can be used for indentation testing. Note that standard NX (D =54 mm) sized cylindrical rock samples are also used for Schmidt hammer and indentation tests. The cylindrical rock sample is smooth and free of irregularities.

When ε_{af} > 1 %, relative errors (Δ) between uniaxial compressive strengths (σ_c) of carbonate rocks defined by standard L-type Schmidt hammer and by uniaxial compressive test are < 18% (Palchik 2012). In case where ε_{af} < 1%, these errors are smaller: Δ = 10%. The values of Δ are smaller than 13% when σ_{a1} and ε_{a1} = 0.05%-0.2% observed by standard punch indentation test and those obtained from uniaxial compression test are compared. When σ_c and one datum point (σ_{a1}, ε_{a1}) defined by Schmidt hammer test and indentation test, respectively, are used as input values in Eqs. (13) and (15), relative errors between calculated (Eqs. (13) and (15)) σ_a and that obtained from uniaxial compressive test are < 12 %.

7. Conclusions

The applicability of exponential stress-strain models for weak-to-strong carbonate rocks (chalks, dolomites and limestones) used for tunnel construction is presented. It is established that exponential stress-strain models (Eqs. (1) and (2)) based on Haldane's distribution function presented in transformed forms (Eqs. (13) and (15), respectively) are suitable for accurate prediction of stress-strain response of carbonate rocks exhibiting small (< 0.5%), intermediate (< 1%) and large (> 1%) axial strains over the whole pre-failure strain range avoiding the use of press machine. The proposed equations (Eqs. (13) and (15)) do not involve the value of ε_{af}, and input parameters for these equations are uniaxial compressive strength (σ_c < 100 MPa) defined using non-destructive standard device (Schmidt hammer) and only one point measurement (0.05% <ε_{a1} < 0.2% and σ_{a1} at this ε_{a1}). The small value of ε_{a1} = 0.05%-0.2% and relatively small applied load (σ_{a1}) are readily defined by indentation test.

Acknowledgements

The author is grateful to two anonymous reviewers for their very useful comments.

References

ASTM. (2001), *Standard Test Method for Determination of Rock Hardness by Rebound Hammer Method*, ASTM Standards, 04.09. (D5873-00)

Bogusz, A. and Bukowska, M. (2015), "Stress-strain characteristics as a source of information on the destruction of rocks under the influence of load", *J. Sustain. Min.*, **14**(1), 46-54.

Brown, E.T. (1981), *Rock Characterization Testing and Monitoring: ISRM Suggested Methods*, Pergamon Press, Oxford, U.K.

Chen, L.H. and Labuz, J.F. (2006), "Indentation of rock by wedge-shaped tools", *Int. J. Rock Mech. Min. Sci.*, **43**(7), 1023-1033.

Ching, L.L., Ta, P.C., Dong, H.Y. and Ching, S.C, (1997), "Stress-strain relationship for granular materials based on hypothesis of best fit", *Int. J. Solid. Struct.*, **34**(31-32), 4087-4100.

Duncan, J.M. and Chang, C.Y. (1970), "Non-linear analysis of stress and strain in soils", *J. Soil Mech. Found. Div.*, **96,** 1629-1653.

Fairhurst, C.E. and Hudson, J.A. (1999), "Draft IRSM suggested method for the complete stress-strain curve for intact rock in uniaxial compression", *Int. J. Rock Mech. Min. Sci.*, **36**(3), 281-289.

Garaga, A. and Latha, G.M. (2010), "Intelligent prediction of the stress-strain response of intact and jointed rocks", *Comput. Geotech.*, **37**(5), 629-637.

Gutierrez, M., Kolderup, U.M. and Hoeg, K. (2000), "Model for 3D time-dependent chalk stress-strain behavior", *Proceedings of the 6th North Sea Symposium*, Brington, UK.

Haas, C.J. (1989), *Static Stress-Strain Relationships*, in *Physical Properties of Rocks and Minerals*, Hemisphere Publishing, Taylor and Francis, London, U.K.

Habimana, J., Labiouse, V. and Decoeudres, F. (2002), "Geomechanical characterisation of cataclastic rocks: Expirence from the Cleuson-Dixence project", *Int. J. Rock Mech. Min. Sci.*, **39**(6), 677-693.

Haftani, M., Bohloli, B., Moosavi, M., Nouri, A., Moradi, M. and Maleki Javan, M.R. (2013), "A new method for correlating rock strength to indentation tests", *J. Petrol Sci. Eng.*, **112,** 24-31.

Haldane, J.B.S. (1919), "The combination of linkage values and the calculation of distances between the loci of linked factors", *J. Genet.*, **8**(29)**,** 299-309.

Hazewinkel, M. (2001), *Taylor Formula: Encyclopedia of Mathematics*, Springer

Kalyan, B., Murthy, Ch.S.N. and Choudhary, R.P. (2015), "Rock indentation indices as criteria in rock excavation technology-A critical review", *Proc. Earth Planet. Sci.*, **11,** 149-158.

Karaman, K. and Kesimal, A. (2015), "A comparative study of Schmidt hammer test methods for estimating the uniaxial compressive strength of rocks", *Bull. Eng. Geol. Environ.*, **74**(2), 507-520.

Kodner, R.B. (1963), "Hyperbolic stress-strain response: Cohesive soils", *J. Soil Mech. Found. Div.*, **89**(1)**,** 115-143.

Kumara, J.J. and Hayano, K. (2016), "Importance of particle shape on stress-strain behaviour of crushed stone-sand mixtures", *Geomech. Eng.*, **10**(4), 455-470.

Li, Y., Zhang, S. and Zhang, B. (2018). "Dilatation characteristics of the coals with outburst proneness under cyclic loading conditions and the relevant applications", *Geomech. Eng.*, **14**(5), 459-466.

Liu, H.H., Rutqvist, J. and Berryman, J.G. (2009), "On the relationship between stress and elastic strain for porous and fractured rock", *Int. J. Rock Mech. Min. Sci.*, **46**(2), 289-296.

Muravskii, G.B. (1996), "On analytical description of stress-strain relationship for rocks and soils", *Commun. Num. Meth. Eng.*, **12**(12), 827-834.

Palchik, V. (2006), "Stress-strain model for carbonate rocks based on Haldane's distribution function", *Rock Mech. Rock Eng.*, **39** (3), 215-232.

Palchik, V. (2007), "Use of stress-strain model based on Haldane's distribution function for prediction of elastic modulus", *Int. J. Rock Mech. Min. Sci.*, **44**(4), 514-524.

Palchik, V. (2012), "Relation between normalized axial stress and failure strain in heterogeneous carbonate rocks exhibiting large axial strains", *Rock Mech. Rock Eng.*, **45**(2), 217-224.

Palchik, V. (2014), "Use of Descartes folium equation for deriving a relation between total aperture of fractures after uniaxial compression and strain parameters of different rocks exhibiting negative total volumetric strain", *Rock Mech. Rock Eng.*, **47**(6), 2075-2086.

Palchik, V. and Hatzor, Y.H. (2000), "Correlation between mechanical strength and microstructural parameters of dolomites and limestones in the Judea group-Israel", *Isr. J. Earth Sci.*, **49**(2), 65-79.

Puzrin, A.M. and Burland, J.B. (1996), "A logarithmic stress-strain function for rocks and soils", *Geotechnique*, **46**(1), 157-164.

Schmidt, E. (1951), "A non-destructive concrete tester", *Concrete,* **59**, 51-54.

Shibuya, S. (2002), "A non-linear stress-stiffness model for geomaterials at small to intermediate strains", *Geotech. Geol. Eng.*, **20**(4), 333-369.

Tatsuoka, F. and Shibuya, S. (1992), "Deformation characteristics of soils and rocks from field and laboratory tests", *Proceedings of the 9th Asian Conference on Soil Mechanics and Foundation Engineering*, Bangkok, Thailand, December.

Tharp, T.M. and Scarbrough, M.G. (1994), "Application of hyperbolic stress-strain models for sandstone and shale to fold wavelength in Mexican Ridges Foldbelt", *J. Struct. Geol.*, **16**(12), 1603-1618.

Yadollahia, M.M. and Benli, A. (2017). "Stress-strain behavior of geopolymer under uniaxial compression", *Comput. Concrete,* **20**(4), 381-389.

CC